Arrays of Interacting Magnetic Dots and Wires: Static and Dynamic Properties

B. Hillebrands, S.O. Demokritov, C. Mathieu, S. Riedling, O. Büttner, A. Frank, B. Roos, J. Jorzick
Fachbereich Physik und Schwerpunkt Materialwissenschaften, Universität Kaiserslautern, 67653 Kaiserslautern, Germany,

A.N. Slavin
Department of Physics, Oakland University, Rochester, MI 48309, U.S.A.

B. Bartenlian, C. Chappert
IEF, Université Paris Sud, 91405 Orsay, France

F. Rousseaux, D. Decanini, E. Cambril
L2M, Bagneux, France

A. Müller, U. Hartmann
Universität Saarbrücken, Germany

Static and dynamic properties of patterned magnetic permalloy films are investigated. In square lattices of circular shaped permalloy dots an anisotropic coupling mechanism has been found, which is identified as being due to intrinsically unsaturated parts of the dots caused by spatial variations of demagnetizing field. In arrays of magnetic wires a quantization of the surface spin wave mode in several dispersionless modes is observed and quantitatively described. For large wavevectors the frequency separation between the modes becomes smaller and the frequencies converge to the dispersion of the dipole-exchange surface mode of a continuous film.

Progress made during the last decade in handling and the analysis of matter leads to the elaboration of well-controlled artificial magnetic structures from micron to nanometer size. These structures, which usually present arrays of separated magnetic items, are attracting increasing interest due to their potential applications in magnetic storage devices and sensors.[1),2),3),4),5)] Fundamental studies of both static and dynamic properties of a single item as well as coupling phenomena between the items in arrays should determine the limits of their possible application. A precise control of magnetic anisotropies induced by patterning processes as well as of the coupling between the items is required. The frequencies and the mode profiles of spin waves propagating in the items are of particular importance for the optimization of the remagnetization process of the items in, e.g., sensor and memory applications.

In this paper we report on the investigation of the static and dynamic properties of regular arrays of magnetic dots and wires by Brillouin light scattering (BLS), Kerr magnetometry and magnetic force microscopy (MFM). Whereas Kerr magnetometry and magnetic force microscopy were used to determine the static magnetic properties of the dots and wires, the spin wave properties were obtained from BLS spectra. On the basis of this comprehensive study we can claim that we have found an anisotropic in-plane coupling mechanism between magnetic dots arranged in a square lattice, which is correlated to intrinsic inhomogeneities of the dot magnetizations. We also observed a quantization effect of spin waves in magnetic wires, which is caused by the finite width of the wires. The evolution of the Damon-Eshbach (DE) surface spin wave mode of a continuous film from the discrete eigenmode spectrum of the wires with increasing wavevector, i.e. with diminishing influence of the finite size effect, is demonstrated and quantitatively described by a model based on quantized modes.

The samples under investigation were regular square lattices of circular shaped dots or periodic arrays of wires, made of permalloy ($Ni_{80}Fe_{20}$). As the first step of the sample preparation, 200, 500, and 1000 Å thick permalloy films were deposited in UHV onto SiO_2/Si(111) 10×10 mm^2 substrates by means of e-beam evaporation. As a reference non-patterned films where studied first. The result is, that the in-plane anisotropy of the non-patterned film is negligble. As the next step the samples were patterned by synchrotron radiation based X-ray lithography performed at the L2M synchrotron station at the super ACO storage at LURE, Orsay, using ion beam etching to transfer the patterns into the permalloy films. The details of the patterning procedure are published elsewhere.[6)] Eight different samples comprising circular dots arranged in a 1x1 mm^2 square lattice with a diameter/periodicity of 1/1.1, 1/2, 2/2.2 and 2/4 µm, respectively, patterned into 500 and 1000 Å thick films, as well as two samples with periodic arrays of wires with a wire width w = 1.8 µm and wire separations of 0.7 and 2.2 µm patterned into a 200 Å thick film were prepared. The length of the wires was 500 µm. The patterned area for each of the two wire samples was 500×500µm^2. Depth profile measurements show that the etching process cuts 250 Å deep into the substrate between the items, which guarantees, that even for the smallest distances neighboring items were not touching.

The magnetization reversal behavior of the structures has been investigated using Kerr magnetometry. Remagnetization loops have been measured as a function of the angle Φ_H of the in-plane applied field with respect to the in-plane

Preprint Server AG Hillebrands: http://www.physik.uni-kl.de/w_hilleb, J. Mag. Soc. Jpn. 23, 670 (1999)

[01]-direction. The domain structure of the dots was studied by magnetic force microscopy (MFM). MFM images have been recorded at an applied field of up to 2 kOe using a vertically magnetized Co-coated Si-cantilever. The spatial resolution was better than 100 nm.

The spin wave properties were investigated by using a computer controlled tandem Fabry-Perot interferometer as described elsewhere.[7] Laser light of a single-moded Ar^+ laser operating at a wavelength of λ_{Laser} = 514.5 nm with a power of up to 50 mW was focused onto the samples, and the frequency spectrum of the backscattered light was analyzed. For the investigation of the anisotropic properties of the dot samples the applied magnetic field can be rotated in the plane of the films. On the contrary, the BLS experiments on wires were performed with a fixed orientation of the applied field along the wire axes. The in-plane wavevector of the spin waves tested in the experiment was always oriented perpendicular to the applied field. Its value is determined by the scattering geometry and can be varied by changing the angle of light incidence, θ, measured against the surface normal, since $q_{\parallel} = (4\pi/\lambda_{Laser}) \cdot \sin\theta$. If necessary, the collection angle of the scattered light was chosen small enough to ensure a reasonable resolution in $q_{\parallel}$ of $\pm 0.8 \cdot 10^4$ cm^{-1}. At small angles of light incidence the directly reflected beam and diffraction reflexes entering the collection lens were blocked by small blinds inserted into the collection aperture.

Figure 1 shows magnetization curves of the wire and dot samples measured for different orientations of the applied field. The two-fold symmetry of the curves reflects the shape anisotropy of the wires and is due to demagnetizing effects. The corresponding saturation fields are in a good agreement with the calculation of the demagnetization factors of the wires, based on the known formulas.[8] As it is also seen, the dot curves, corresponding to large interdot distances (1/2 μm lattice) are similar for both field directions, which also agrees with the demagnetizing field calculation of a single dot. In fact, the in-plane demagnetizing tensor of a circular dot is a scalar. On the other hand, a fourfold in-plane anisotropy in the loop shapes is found for the lattices with the smallest dot separation of 0.1 μm (1/1.1 μm lattice).

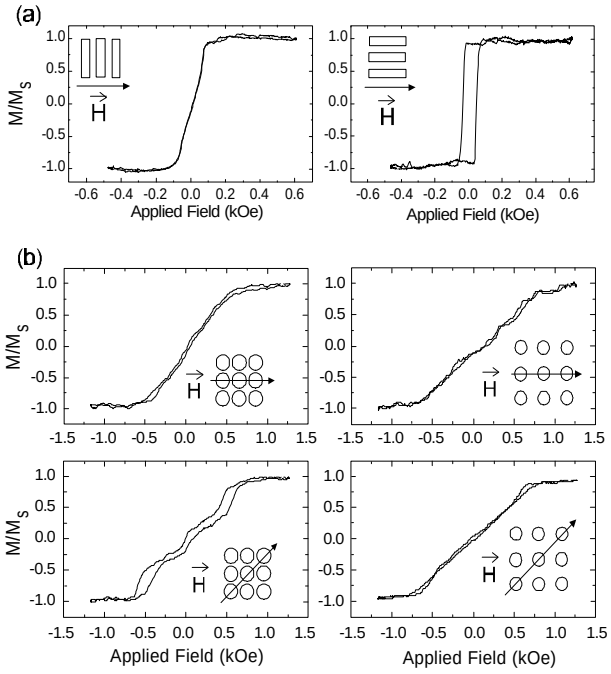

Fig. 1: Magnetization curves for different field orientations of a) the wire sample with the distance between wires of 2.2 μm and b) of the 1/1.1 μm (left) and 1/2 μm (right) dot samples of 1000 Å dot thickness.

Actually, the loop shape of the 1/1.1 μm lattice along the [10]-direction is very similar to the loop shapes of the 1/2 μm lattices for all field directions. In contrary, the loop shape of the 1/1.1 μm lattice with *H* along the [11]-direction is rather complex. Similar loop shapes have been obtained by Smyth et al.,[1] but the magnetization reversal process is not yet understood. Since these loop shapes exhibit a higher zero-field susceptibility, they indicate that the [11]-direction of the lattice is the easy axis. The magnetization curves of the dot lattices demonstrate the fact that in the 1/1.1 μm lattice the coupling between dots becomes important.

A direct proof of such a coupling is yielded by magnetic force microscopy. MFM-images of the 1/1.1 μm lattice of 500 Å thickness for different values of the magnetic field are shown in Fig. 2. For all values of the applied field below 1 kOe a heterogeneous magnetic structure is clearly recognizable, which seems not to be totally disordered. Radial domain walls corresponding to flux-closure domains are observed. For $H = 0$ a regular pattern of domain walls can be seen, which are aligned cross-like along the [10]-direction,. This is clear evidence for a coupling between the dots. Since the 1/2 μm lattice demonstrates no order in the orientation of the domain walls (see, e.g. Ref. 5), one can conclude that this coupling is only effective for small dot

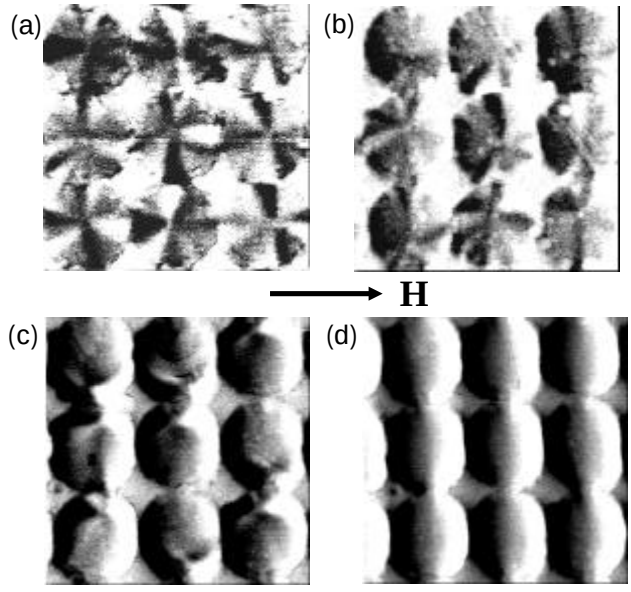

Fig. 2: MFM images of the 1/1.1 μm dot sample of 500 Å thick dots for different values of the magnetic field applied horizontally a) $H = 0$, b) $H = 300$ Oe, c) $H = 600$ Oe and d) $H = 1.5$ kOe. The black/white contrast is determined by the vertical component of stray fields. Note the cross-like order of domain walls along the [10] direction at $H = 0$.

separations. One also can see in Fig. 2(a) an order in the magnetization of the walls itself. Due to a vertical magnetization of the cantilever the white and black contrast in Fig. 2 corresponds to vertically oriented stray fields or vertical components of the magnetization in the wall. There is a degeneracy in the orientation of these components. On the other hand, it is clearly seen, that adjoing walls exhibit mostly opposite vertical magnetizations, which agrees with the minimum of the magneto-dipole interaction between these magnetization components. With increasing applied field the intersections of the domain walls in different dots move either up or down, indicating clockwise or counterclockwise rotation of the magnetization in flux closure domains in the corresponding dots.

Of particular interest are the dynamic properties of these patterned structures. A detailed BLS study of the dependence of the spin wave properties on the applied magnetic field has been performed. All Brillouin light scattering spectra display clearly peaks corresponding to surface magnetic excitations (Damon-Eshbach-mode).[9] The wire samples exhibit a multiple splitting of this peak, whereas in the case of the dot samples one observes no splitting. The former case is connected with the lateral quantization of spin waves in wires. It will be considered in detail in the last part of the paper. Let us first consider the results obtained on the dot samples. The measured spin wave frequencies of the different dot arrays as a function of the applied field are shown in Fig. 3. For each dot array the spin wave frequencies decrease with decreasing field, and they disappear below certain critical applied fields. The strong reduction of the spin wave frequencies with decreasing aspect ratio is also seen in Fig. 3. This is caused by size depending demagnetizing fields as follows: The frequency of the DE-mode can be expressed as[9]

$$\nu = \frac{\gamma}{2\pi}\cdot\left[H_i\cdot\left(H_i+4\pi M_s\right)+\left(2\pi M_s\right)^2\cdot\left(1-e^{-2q_{\|}d}\right)\right]^{1/2} \tag{1}$$

with γ the gyromagnetic ratio, M_s the saturation magnetization, $q_{\|}$ the in-plane wavevector, and d the film thickness. H_i is the internal field, which is here defined as

$$H_i = H + \beta H_a - N\cdot 4\pi M_s \tag{2}$$

with N the demagnetizing factor of the magnetic dots, decreasing with their aspect ratio, and H_a the anisotropy field. The factor β depends on the orientation of the applied field relatively to the easy axis: $\beta = 1$, if the field is applied along the easy axis and $\beta = -1$, if the field is applied along the hard axis. The Eq. (1) presumes a saturation of the in-plane magnetization of the sample. The solid lines in Fig. 3 are calculated on the basis of Eq. (1) using demagnetizing factors of spheroids with axial ratios taken from the aspect ratios of the magnetic dots. They are in reasonably good agreement with the experimental data for $H > N\times 4\pi M_s$.

To clarify the problem of an anisotropic in-plane interdot coupling, we measured the spin wave frequencies of the DE-mode as a function of the angle of the in-plane applied field,

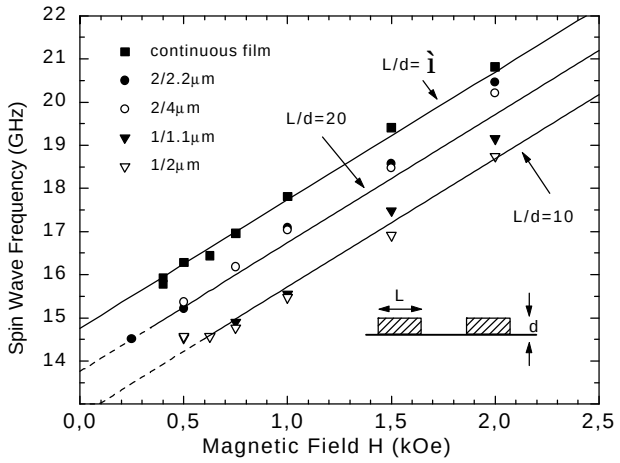

Fig. 3: Measured spinwave frequencies of different dot samples of 1000 Å dot thickness as a function of the applied field. The solid lines represent the calculated frequencies on the basis of Eqs. (1) and (2) using aspect ratios as indicated.

Φ_H, with respect to a reference [10]-direction of the lattice. The results are displayed in Fig. 4 for the 1/1.1 µm and, for comparison, for the 1/2 µm dot lattices of the sample of 1000 Å thickness at an applied field of 1 kOe. Again, only for the smallest dot separations of 0.1 µm a fourfold anisotropic dependence $\nu(\Phi_H)$ is found. To determine quantitatively the anisotropy constant we use the energy expression

$$F = K^{(4)}\sin^2\Phi\cdot\cos^2\Phi \tag{3}$$

with Φ the angle between the direction of magnetization with respect to the [10]-direction, and $K^{(4)}$ a fourfold in-plane anisotropy constant. A model fit using Eq. (3) and a numerical procedure to calculate the spinwave frequencies[10] is displayed in Fig. 4 as a solid line for the 1/1.1 µm lattice. The obtained value of the anisotropy contribution $K^{(4)}$ was found to be dependent on the applied magnetic field. For both 1/1.1 µm samples with thicknesses of 500 Å and 1000 Å $K^{(4)}$ was determined for several values of the field strength. The obtained results are as follows: $K^{(4)} = -2\cdot 10^5$ erg/cm^3 at low fields, and it decreases with increasing field down to $K^{(4)} = -0.6\cdot 10^5$ erg/cm^3 at H=3-5 kOe For the sample with higher aspect ratio, one needs a higher value of the applied field to reach a given reduction of $K^{(4)}$.

On the basis of the above experimental data the origin of this fourfold anisotropy can be understood as being caused by a magneto-dipole interaction between residual unsaturated parts of the dots. Because of the large distance of 0.1 µm between the dots a direct exchange mechanism via conduction electrons or via electron tunneling can be excluded. The quasi-uniform demagnetizing field, caused by the shape of the patterned area (1x1 mm^2 square) cannot be responsible for the observed anisotropy. In fact, the film thickness/square length ratio is of the order of 10^4. It corresponds to a demagnetizing field of about 1 Oe, which is much smaller than the observed value of the anisotropy field of 150 Oe. Moreover, since the quasi-uniform field strength should depend on the average magnetization of the lattice, the effect

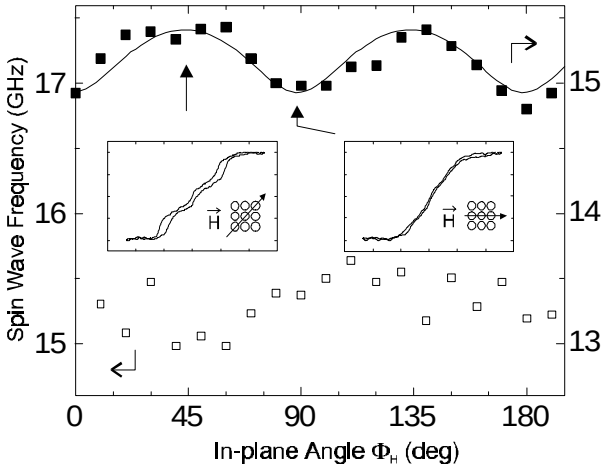

Fig. 4: Dependence of the spinwave frequencies on the in-plane direction of the applied field for the 1/1.1 µm (■) and, for comparison, for the 1/2 µm (□) dot samples of 1000 Å thickness. The solid line is a fit for the data (see text). Magnetization curves of the 1/1.1 µm dot lattice are shown as insets with the applied field as indicated. Note that a maximum values of the spin-wave frequency corresponds to an easy axis.

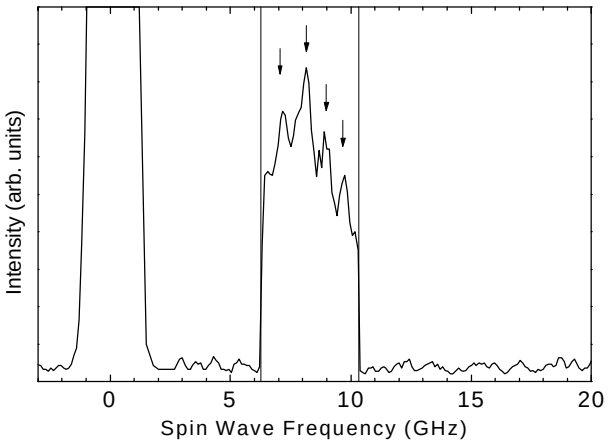

Fig. 5: Brillouin light scattering spectrum of the wire sample with a wire width of 1.8 µm and a wire separation of 2.2 µm, demonstrating the existence of several discrete spin wave modes with a mode splitting of about 0.9 GHz (indicated by arrows). The applied field H=0.5 kOe is along the wire axes. The in-plane wavevector $q_{||} = 0.3 \cdot 10^5$ cm^{-1} is perpendicular to the wire axes.

should be the same for the 1/1.1 µm and 2/2.2 µm lattices, which is not the case. A dipolar interaction of completely magnetized dots also cannot account for the observed anisotropy, because the corresponding dipolar energy can be expressed as a bilinear form of the components of the magnetization vector. Such an expression can only yield an uniaxial, but not a fourfold anisotropy contribution, since in a bilinear form the direction cosines appear quadratic in highest order and add to a constant if a fourfold symmetry is given. But, if the dots are not completely saturated, the magneto-dipole interaction energy cannot be expressed in the above bilinear form, and the fourfold anisotropy is not theoretically forbidden. The large observed decrease of the coupling anisotropy constant with increasing field corroborates this assumption. However, the anisotropic coupling is still observed for high fields where according to the magnetization curves the saturation should be reached. It is not so much surprising, because the MFM-images show that the non-saturated parts of the dots can persist up to fairly high fields, probably due to an intrinsic inhomogeneity, as it might be caused, e.g., by surface anisotropy contributions at the side walls of the dots.

As it was already mentioned, the peaks in the BLS spectra of the wire samples, which correspond to surface magnetic excitations, demonstrate multiple splitting. As an example, the anti-Stokes side of a typical Brillouin light scattering spectrum for a wavevector $q_{||} = 0.3 \cdot 10^5 cm^{-1}$ of the sample with 1.8 µm separation between the wires is shown in Fig. 5. Near 7.1, 8.0, 8.8 and 9.6 GHz four distinct modes of magnetic excitations are observed. For understanding this phenomenon the dispersion relation, $n(q_{||})$ of the spinwave frequencies was carefully studied. The obtained results are displayed in Fig. 6. Shown are the data for the wires with a separation of 2.2 µm (solid symbols), and 0.7 µm (open symbols). In the region of low wavevectors the spin wave modes show a disintegration of the continuous dispersion of the DE-mode into several discrete modes with frequencies of the lowest lying modes of 7.1, 8.0, 8.8, 9.6, and 10.2 GHz with an experimental error of ±0.1 GHz. There is no significant difference between the data obtained from the wires with 0.7 and 2.2 µm separation, indicating that the mode

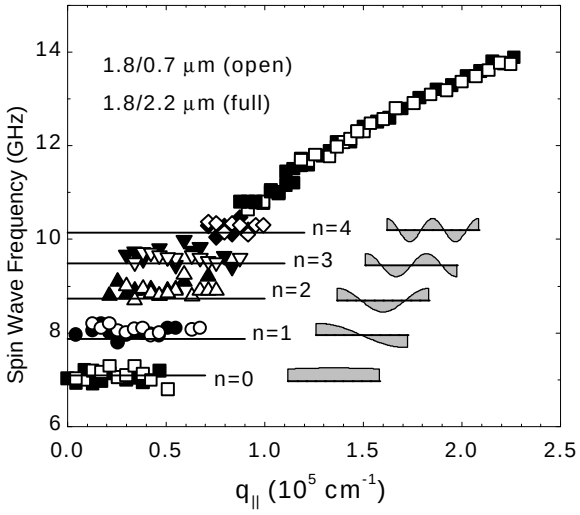

Fig. 6: Obtained spin wave dispersion curves for an array of wires of 1.8 µm width and a separation of the wires of 2.2 µm (solid symbols) and 0.7 µm (open symbols). The thickness of the wires is 200 Å, the external field applied along the wire axes is 0.5 kOe. For comparison the frequencies of the five lowest quantized surface spin wave modes, n = 0–4, calculated on the basis of Eqs.(1) and (6) are also shown (horizontal lines). Bottom right: magnetization profiles of these modes calculated using Eqs. (5) and (6) as described in the text.

splitting is purely caused by the quantization of the spin waves due to the finite wire width, and the magneto-dipole interaction between wires is small for both separations studied. The main features of the dispersion law, observed in the entire studied interval of $q_{\|}$ shown in Fig. 6 are as follows: (i) For low wavevector values ($\cong 0 - 0.9\cdot10^5$ cm^{-1}) discrete modes, showing no noticeable dependence of their frequencies on $q_{\|}$ exist. (ii) The lowest mode appears near zero wavevector ($|q_{\|}| \le 0.08\cdot10^5$ cm^{-1}), whereas all higher modes appear at higher wavevectors, and the value of the respective lower "cut-off" wavevector increases with the mode number. (iii) For large values of the wavevector ($q_{\|} > 1.3\cdot10^5$ cm^{-1}) the dispersion of the patterned film converges to that of a continuous film. (iv) There is a transition region, where due to the small mode separation, which is close or slightly below the experimental frequency resolution in the BLS experiment ($\approx$ 0.1 GHz), the modes can be hardly resolved.

In an infinite ferromagnetic film of thickness d with the direction of magnetization aligned perpendicular to the spin-wave wavevector and within the film plane, the dipole-exchange spin wave spectrum of the film consists of the surface, dipole-dominated DE-mode (see. Eq.(1)) and the higher frequency exchange-dominated modes with large perpendicular wavevector components, $q_{\perp}$, taking the quantized values of $k\pi/d$ with k = 1,2,3, …. Although these exchange-dominated modes are also observed in our experiments, they are not further considered here since their frequencies, which are much higher than the frequencies of the discrete modes, depend only on the film thickness (and *not* on the in-plane pattern parameters).

To calculate the mode frequencies and profiles for the array of wires we assume in the following a Cartesian coordinate system oriented such that the normal of the patterned area points into the x-direction, the wavevector $q_{\|}$ points into the y-direction, and the wire axes, and the applied magnetic field and the magnetization are all aligned parallel to the z-axis. In the case of small values of $q_{\|}$ it is natural to assume that the observed discrete spin wave modes result from the width-dependent quantization of the in-plane wavevector q_n in the DE-dispersion equation, described by Eq. (1) with demagnetizing field $H_d = 0$ since the magnetic field is applied along the wires and the aspect ratio in this case is very high. The quantized values of q_n in a thin ($d << w$) magnetic wire of thickness d and width w can be obtained by imposing boundary conditions on the variable magnetization m at the side walls of the wire (see, e.g., Refs. 11,12). For the boundary conditions $\partial m/\partial y\big|_{y=\pm w/2} = 0$, corresponding to zero surface anisotropy, we obtain equidistant values $q_n = n\pi/w$, where n = 0,1,2, ... Discrete spin wave mode frequencies can be obtained by substituting these values of q_n along with the independently measured parameters of our sample (d = 200 Å, w = 1.8 μm, $4\pi M_S$ = 10.2 kG, H = 0.5 kOe, $\gamma/2\pi$ = 2.95 GHz/kOe) into the dispersion equation Eq. (1) : ν_0 = 6.82, ν_1 = 7.86, ν_2 = 8.72, ν_3 = 9.45, and ν_4 = 10.08 GHz. It is evident from the comparison with the experimentally measured values, that for $n > 0$ the calculated mode frequencies are in good quantitative agreement with our experimental results. We also note, that the frequency separation $\Delta\nu = \nu_{n+1} - \nu_n$ of the discrete modes, as observed in our experiment, decreases with increasing wavenumber, q_n, in agreement with our calculations. This is due to the fact that the group velocity $V_g = \partial\omega/\partial q$ of the dipolar surface spin wave (cf. Eq. (1)) decreases with increasing wavevector. Thus the frequency splitting of neighboring, width-dependent discrete spin wave modes, which are equally separated in the q-space ($q_n = n\pi/w$), becomes smaller with increasing wavevector q_n, until the mode separation is smaller than the frequency resolution in the BLS experiment and/or the natural line width and the splitting is not anymore observable. In this regime the observed spin wave spectrum is well described by the dispersion equation for a film of infinite width and continuous values of $q_{\|}$. The calculated dispersion curve based on Eq. (1) deviates at the upper end of the measured wavevector region by -0.4 GHz from the experimental values. This problem is easily solved by taking the bulk exchange interaction of permalloy into account (exchange constant $A = 1\cdot10^{-6}$ erg/cm), using, instead of Eq.(1), a full model for the calculation of the dipole-exchange dispersion equation of the surface spin wave mode.[10] Exchange interaction, which is only important at high values of the wavevector, does not significantly affect the frequency positions of the five lowest discrete modes of wires, but it shifts the tail of the calculated dispersion curve to match the experimental values at large q_n.

However, the calculated frequency of the lowest discrete mode of ν_0 = 6.82 GHz is about 0.3 GHz lower than the experimental value of 7.1 GHz. This difference is three times larger than the experimental frequency resolution of 0.1 GHz. To understand the frequency position of the lowest (n = 0) mode we assume that a weak, but finite, surface anisotropy in permalloy creates a weak pinning of the variable magnetization, m, at the side walls of the wire. In analogy to the Rado-Weertman boundary condition at the surfaces of a free film[11] the boundary conditions at the side walls can be written as:

$$\pm\frac{\partial m}{\partial y} + Dm\big|_{y=\pm w/2} = 0\,, \qquad (4)$$

where $D = K_s/A$ is the "pinning" parameter, defined as a ratio of surface anisotropy constant, K_s, to the exchange constant, A.

The magnetization distributions for the discrete width modes, corresponding to the boundary condition Eq. (4), are described by the equation (see, e.g., Ref. 12,13):

$$m_n(y) = a_n\left[\cos\left(q_n(y + w/2)\right) + \sin\left(q_n(y + w/2)\right)D/q_n\right],$$
$$-w/2 < y < w/2. \qquad (5)$$

Substituting Eq. (5) into Eq. (4), we obtain a transcendental equation determining the discrete values of the lateral wavevector q_n :

$$\tan(q_n w) = \frac{2q_n D}{q_n^2 - D^2} \qquad (6)$$

The roots q_n of Eq. (6), substituted in Eq. (1), determine the frequencies of the modes. Using D as an adjustable parameter we obtain the frequency of the lowest mode as ν_0 = 7.1 GHz for $D = 3{\cdot}10^3$ cm^{-1} ($K_s = 3{\cdot}10^{-3}$ erg/cm). The corresponding mode wavevector is $q_0 = 0.5{\cdot}10^4$ cm^{-1}. The calculated values of the mode frequencies, if both weak pinning and exchange are taken into account, are ν_0 = 7.10, ν_1 = 7.87, ν_2 = 8.74, ν_3 = 9.49, and ν_4 = 10.15 GHz. They are shown in Fig. 6 as solid lines. It is clear from Fig. 6 that there is an excellent agreement between these values and the experiment. The magnetization profiles (see Eq. (5)) along the wire width of these modes are also depicted in Fig. 6 (right). Note here, that the value of D, needed to shift the frequency of the lowest mode to match the experiment, is so small, that it practically does not affect the frequency positions and magnetization distributions of the higher (n > 0) discrete modes, since $D/q_n << 1$ for $n > 0$ and therefore the corrected values of q_n are very close to $q_n = n\pi / w$.

Above interpretation of the observed discrete modes is further supported by the data of the wavevector intervals in which the modes can be observed. Due to the momentum conservation law an infinite traveling plane wave contributes to the inelastic light scattering process at a definite value of $q_\parallel$, or, in our geometry, at a definite angle of light incidence, θ. On the other hand, the spin wave modes under investigation are restricted in space, since they only exist in the wire of width w and their amplitude is zero outside the wire. The light scattering process for such modes takes place within a certain interval of θ, and the scattering intensity is determined by the respective Fourier component $m(q_\parallel)$ of the mode: $I \propto |m(q_\parallel)|^2$. These calculated Fourier component profiles should clearly define the intervals of $q_\parallel$, in which the corresponding spin wave modes should be detectable.

The calculated intensity profiles $|m_n(q_\parallel)|^2$ for the discrete modes (see Eq. (5)) show maxima near q_n and their widths along the $q_\parallel$-axis are about $\pm \pi/w$ ($\pm 2{\cdot}10^4$ cm^{-1}). There is a good agreement between the results of this calculation and the experimentally measured wavevector intervals, where the corresponding discrete modes are observed, if especially one takes into account the experimental uncertainty of $q_\parallel$, caused by a finite, albeit small, collection aperture.

In summary, we have investigated static and dynamic magnetic properties of arrays, consisting of permalloy dots and wires by means of Kerr magnetometry, magnetic force microscopy and Brillouin light scattering. We have revealed clear evidence for a fourfold in-plane anisotropic coupling of magnetic micron dots, mediated by stray fields of non-saturated parts of the dots. The frequencies of the spin waves observed in dots and wires can be well described by a modified Damon-Eshbach equation. We have found a spin wave mode quantization effect in a periodic array of magnetic wires. The observed discrete modes can be interpreted as resulting from the width-dependent quantization of the dipole-dominated surface spin wave mode (quasi-DE-mode) of an infinite film. Both the frequency positions and the wavevector intervals, where the discrete modes are observed, support our interpretation. No indication for a zone folding effect due to the periodic arrangement of the wires was found.

Acknowledgments: Support by the Deutsche Forschungsgemeinschaft and the National Science Foundation of the U.S.A. is gratefully acknowledged.

References

1) J.F. Smyth, S. Schultz, D. Kern, H. Schmidt, D. Yee: *J. Appl. Phys.* **63**, 4237, (1988).
2) B.A. Gurney, P. Baumgart, V. Speriosu, R. Fontana, A. Patlac, T. Logan, P. Humbert: *Digest of the International Conf. on Magnetic Films and Surfaces*, Glasgow, (1991).
3) A. Maeda, M. Kume, T. Ogura, K. Kukori, T. Yamada, M. Nishikawa, and Y. Harada: *J. Appl. Phys.* **76**, 6667 (1994).
4) B. Hillebrands, C. Mathieu, M. Bauer, S.O. Demokritov, B. Bartenlian, C. Chappert, D. Decanini, F. Rousseaux, and F. Carcenac: *J. Appl. Phys.* **81**, 4993 (1997).
5) C. Mathieu, C. Hartmann, M. Bauer, O. Büttner, S. Riedling, B. Roos, S.O. Demokritov, and B. Hillebrands: *Appl. Phys. Lett.* **70**, 2912 (1997).
6) F. Rousseaux, D. Decanini, F. Carcenac, E. Cambril, M.F. Ravet, C. Chappert, N. Bardou, B. Bartenlian, P. Veillet: *J. Vac. Technol.* **B 13**, 2787 (1995).
7) R. Mock, B. Hillebrands, and J.R. Sandercock: *J. Phys. E* **20**, 656 (1987). B. Hillebrands: submitted to *Rev. Sci. Instr.*
8) J.A. Osborn: *Phys. Rev.* **67**, 351 (1945)
9) R.W. Damon, J.R. Eshbach: *J. Phys. Chem. Solids* **19**, 308 (1961).
10) B. Hillebrands: *Phys. Rev.* B **44**, 530 (1990).
11) G.T. Rado, J.R. Weertman: *J. Phys. Chem. Solids* **11**, 315 (1959).
12) A.G. Gurevich and G.A. Melkov, Magnetization Oscillations and Waves (CRC Press, New York, 1996).
13) R.F. Soohoo, Magnetic Thin Films, Harper & Row, New York, 1964.